SMC-TR-03-XX

AEROSPACE REPORT NO.
TR-2003(8555)-1

Line Shapes of Atomic-Candle-Type Rabi Resonances

31 December 2002

Prepared by

J. C. CAMPARO,[1] J. G. COFFER,[1] B. SICKMILLER,[1,2]
and A. PRESSER[1,3]

[1]Photonics Technology Department, Laboratory Operations
The Aerospace Corporation, Los Angeles, CA
[2]Physics Department
Whittier College, Whittier, CA
[3]Henry Samueli School of Engineering and Applied Science
University of California, Los Angeles, CA

Prepared for

SPACE AND MISSILE SYSTEMS CENTER
AIR FORCE SPACE COMMAND
2430 E. El Segundo Boulevard
Los Angeles Air Force Base, CA 90245

Engineering and Technology Group

THE AEROSPACE CORPORATION
El Segundo, California

This report was submitted by The Aerospace Corporation, El Segundo, CA 90245-4691, under Contract No. F04701-00-C-0009 with the Space and Missile Systems Center, 2430 E. El Segundo Blvd., Los Angeles Air Force Base, CA 90245. It was reviewed and approved for The Aerospace Corporation by B. Jaduszliwer, Principal Director, Electronics and Photonics Laboratory. Michael Zambrana was the project officer for the Mission-Oriented Investigation and Experimentation (MOIE) program.

This report has been reviewed by the Public Affairs Office (PAS) and is releasable to the National Technical Information Service (NTIS). At NTIS, it will be available to the general public, including foreign nationals.

This technical report has been reviewed and is approved for publication. Publication of this report does not constitute Air Force approval of the report's findings or conclusions. It is published only for the exchange and stimulation of ideas.

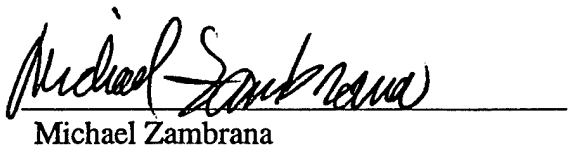

Michael Zambrana
SMC/AXE

REPORT DOCUMENTATION PAGE

Form Approved
OMB No. 0704-0188

1. REPORT DATE (*DD-MM-YYYY*)	2. REPORT TYPE	3. DATES COVERED (*From - To*)
31/12/2002		

4. TITLE AND SUBTITLE
Line Shapes of Atomic-Candle-Type Rabi Resonances

5a. CONTRACT NUMBER
F04701-00-C-0009

5b. GRANT NUMBER

5c. PROGRAM ELEMENT NUMBER

6. AUTHOR(S)
J. C. Camparo, J.G. Coffer, B. Sickmiller, and A. Presser

5d. PROJECT NUMBER

5e. TASK NUMBER

5f. WORK UNIT NUMBER

7. PERFORMING ORGANIZATION NAME(S) AND ADDRESS(ES)

The Aerospace Corporation
Laboratory Operations
El Segundo, CA 90245-4691

Physics Department
Whittier College,
13406 E. Philadelphia,
Whittier, CA 90608

H. Samueli School of Engineering
and Applied Science, UCLA
LA, CA 90095

8. PERFORMING ORGANIZATION REPORT NUMBER
TR-2003(8555)-1

9. SPONSORING / MONITORING AGENCY NAME(S) AND ADDRESS(ES)
Space and Missile Systems Center
Air Force Space Command
2450 E. El Segundo Blvd.
Los Angeles Air Force Base, CA 90245

10. SPONSOR/MONITOR'S ACRONYM(S)
SMC

11. SPONSOR/MONITOR'S REPORT NUMBER(S)
SMC-TR-03-10

12. DISTRIBUTION/AVAILABILITY STATEMENT

Approved for public release; distribution unlimited.

13. SUPPLEMENTARY NOTES

14. ABSTRACT

When atoms interact with a phase-modulated field, the probability of finding the atom in the excited-state oscillates at the second harmonic of the modulation frequency, $2\omega_m$. The amplitude of this oscillating probability is a resonant function of the Rabi frequency Ω, and this is termed a β Rabi resonance. In this work, we examine the line shape of the β Rabi-resonance both theoretically and experimentally. We find that a small-signal theory of the β-Rabi-resonance condition captures much of the line shape's character, and, in particular, that the resonance's "line Q" (i.e., $2\delta\Omega_{1/2}/\Omega$) is proportional to the modulation frequency. This result can be applied to the atomic candle, where β Rabi resonances are employed to stabilize field strength. Considering our results in the context of developing an optical atomic candle, we find that a free-running diode laser's intensity noise could be improved by orders of magnitude using the atomic candle concept.

15. SUBJECT TERMS

16. SECURITY CLASSIFICATION OF:			17. LIMITATION OF ABSTRACT	18. NUMBER OF PAGES	19a. NAME OF RESPONSIBLE PERSON
					J. C. Camparo
a. REPORT	b. ABSTRACT	c. THIS PAGE			19b. TELEPHONE NO. *(include area code)*
UNCLASSIFIED	UNCLASSIFIED	UNCLASSIFIED		7	(310)336-6944

Note

The material reproduced in this report originally appeared in *Physical Review*. The ATR is published to document the work for the corporate record.

J. C. Camparo, J. G. Coffer, B. Sickmiller, and A. Presser, *Physical Review*, Vol. A, No. **66**, 023806 (2002), Pages 023806-1 - 023806-7,

Acknowledgments

The authors thank S. Moss and B. Jaduszliwer for readings of the manuscript and several stimulating discussions.

Line shapes of atomic-candle-type Rabi resonances

J. G. Coffer,[1] B. Sickmiller,[1,2] A. Presser,[1,3] and J. C. Camparo[1]

[1]*Electronics and Photonics Laboratory, The Aerospace Corporation, M2-253, P.O. Box 92957, Los Angeles, California 90009*

[2]*Physics Department, Whittier College, 13406 East Philadelphia, Whittier, California 90608*

[3]*Henry Samueli School of Engineering and Applied Science, University of California, Los Angeles, California 90095*

(Received 11 March 2002; published 8 August 2002)

When atoms interact with a phase-modulated field, the probability of finding the atom in the excited-state oscillates at the second harmonic of the modulation frequency, $2\omega_m$. The amplitude of this oscillating probability is a resonant function of the Rabi frequency Ω, and this is termed a β Rabi resonance. In this work, we examine the line shape of the β Rabi resonance both theoretically and experimentally. We find that a small-signal theory of the β-Rabi-resonance condition captures much of the line shape's character, and, in particular, that the resonance's "line Q" (i.e., $2\delta\Omega_{1/2}/\Omega$) is proportional to the modulation frequency. This result can be applied to the atomic candle, where β Rabi resonances are employed to stabilize field strength. Considering our results in the context of developing an optical atomic candle, we find that a free-running diode laser's intensity noise could be improved by orders of magnitude using the atomic candle concept.

DOI: 10.1103/PhysRevA.66.023806 PACS number(s): 42.62.Fi, 32.70.Jz, 42.62.Eh

I. INTRODUCTION

As has been known for quite some time [1], when an atom interacts with a phase-modulated resonant field, the probability of finding the atom in the excited state, P_e, oscillates. In general, since this probability is a nonlinear function of the resonant field's frequency, the oscillatory behavior of P_e can be quite complicated [2]. However, under typical experimental conditions (as will be discussed more fully below) $P_e(t)$ is well described in terms of just the modulation frequency ω_m and its second harmonic, so that

$$P_e(t)=p_\alpha \sin(\omega_m t+\phi_\alpha)+p_\beta \sin(2\omega_m t+\phi_\beta), \quad (1)$$

where p_α and p_β are oscillation amplitudes that depend on various modulation and atomic parameters. Near resonance, p_α is proportional to the field-atom detuning Δ, so that when the field is exactly on-resonance the probability oscillates at $2\omega_m$.

Belying the deceptively simple appearance of Eq. (1) is the fact that there is no generally valid closed-form expression for p_α and p_β. This is of particular significance in the case of atomic clocks, where the Rabi frequency Ω, the modulation frequency, and the atom's intrinsic dephasing rate γ_2 are all on the same order of magnitude. Consequently, in recent years there have been various attempts to examine the modulated field-atom interaction problem from a broader perspective [3], and, in general, there has been a growing appreciation for the scientific and technological importance of this problem [4–7]. Of relevance for the present discussion are recent studies examining the *resonant* behavior of the p_α and p_β amplitudes, when $\Omega=\omega_m$ and $\Omega=2\omega_m$, respectively [8]; these resonant enhancements in the oscillation amplitudes are termed Rabi resonances; specifically, the α and β Rabi resonances.

While interesting in their own right, the Rabi resonances have a technological application. In particular, in recent studies it was shown that the β Rabi resonance could be used to stabilize the *amplitude* of an electromagnetic field in much the same way as the frequency of a field is stabilized to a resonant transition between energy eigenstates in an atomic clock [9,10]. For ease of reference, and by analogy to the atomic clock, the device exploiting the β Rabi resonance in this manner has been termed an "atomic candle." While the atomic candle's original application was in the area of smart-clock technology [11], recent work has shown that the device can be used to make precise measurements of absorption coefficients and indices of refraction [12], and that it may find application in measuring electromagnetic-field strength in terms of time [13].

In the present work we consider the line shape and linewidth ($2\delta\Omega_{1/2}$) of the β Rabi resonance. In Sec. II, we present a small-signal theory of the Rabi-resonance phenomena, demonstrating the existence of two distinct Rabi resonances (i.e., the α and β resonances). Additionally, we consider the influence of inhomogeneous broadening on the β Rabi resonance, since this can arise when atoms are unable to sample the resonant field's spatial mode structure on the time scale of a Rabi period. Of particular interest in this section will be the atomic line Q of the β Rabi resonance (i.e., $\Omega_0/2\delta\Omega_{1/2}$, where Ω_0 is the resonant Rabi frequency), since this parameter, in combination with the signal-to-noise ratio, determines an atomic candle's stability. In Sec. III we describe our experiment and our results verifying the small-signal theory. Finally, in Sec. IV we consider the implications of our work with regard to the development of an *optical* atomic candle.

II. THEORY

A. Density-matrix evolution

In order to describe the Rabi-resonance phenomenon, we consider the density-matrix equations describing the interaction of a two-level atom with a phase-modulated field [i.e., $\dot{\theta}=m\omega_m\cos(\omega_m t)$, where m is the modulation index], and we consider a small-signal solution for the density-matrix elements, σ_{ij} [10]. Specifically, we let $\sigma_{ij}=\langle\sigma_{ij}\rangle+\delta_{ij}$, where

the $\langle\sigma_{ij}\rangle$ represent unmodulated density-matrix evolution and the δ_{ij} are modulated additions to the density-matrix elements' evolution:

$$(\langle\dot{\sigma}_{ee}\rangle+\dot{\delta}_{ee})=-\gamma_1(\langle\sigma_{ee}\rangle+\delta_{ee})+\Omega\,\mathrm{Im}[\langle\sigma_{eg}\rangle+\delta_{eg}], \tag{2a}$$

$$(\langle\dot{\sigma}_{eg}\rangle+\dot{\delta}_{eg})=-\gamma_2(\langle\sigma_{eg}\rangle+\delta_{eg})+i(\dot{\theta}+\Delta)(\langle\sigma_{eg}\rangle+\delta_{eg})-\frac{i\Omega}{2}[2(\langle\sigma_{ee}\rangle+\delta_{ee})-1]. \tag{2b}$$

Here, γ_1 and γ_2 are the longitudinal and transverse relaxation rates, respectively, Δ is the average field-atom detuning, and we have normalized the density matrix so that $\sigma_{gg}+\sigma_{ee}=1$. To proceed, Eqs. (2) are decomposed into two sets of equations, one for the $\langle\sigma_{ij}\rangle$ and the other for the δ_{ij}. Solving for the unmodulated evolution in steady-state yields

$$\langle\sigma_{ee}\rangle=\frac{1}{2}\left[\frac{(\gamma_2/\gamma_1)\Omega^2}{\gamma_2^2+\Delta^2+(\gamma_2/\gamma_1)\Omega^2}\right], \tag{3a}$$

$$\langle\sigma_{eg}\rangle=-\frac{1}{2}\left[\frac{\Omega(\Delta-i\gamma_2)}{\gamma_2^2+\Delta^2+(\gamma_2/\gamma_1)\Omega^2}\right]. \tag{3b}$$

Solving for the δ_{ij}, we obtain

$$\ddot{\delta}_{ee}+\gamma_1\dot{\delta}_{ee}+\Omega^2\delta_{ee}=-\Omega\gamma_2\,\mathrm{Im}[\delta_{eg}]+\Omega(\dot{\theta}+\Delta)\mathrm{Re}[\delta_{eg}]+\Omega\dot{\theta}\,\mathrm{Re}[\langle\sigma_{eg}\rangle] \tag{4a}$$

and

$$\dot{\delta}_{eg}=-\gamma_2\delta_{eg}+i(\dot{\theta}+\Delta)\delta_{eg}-i\Omega\delta_{ee}+i\dot{\theta}\langle\sigma_{eg}\rangle. \tag{4b}$$

In order to simplify Eqs. (4), we consider a situation in which $|\dot{\theta}|\sim m\omega_m$ is much greater than Δ and γ_2. (Note for later reference that this does not preclude the condition $m\ll 1$.) Then, under the small-signal assumption that $\mathrm{Im}[\langle\sigma_{eg}\rangle]>\mathrm{Im}[\delta_{eg}]$, Eqs. (4) become

$$\ddot{\delta}_{ee}+\gamma_1\dot{\delta}_{ee}+\Omega^2\delta_{ee}\cong\Omega\dot{\theta}[\mathrm{Re}(\langle\sigma_{eg}\rangle)+\mathrm{Re}(\delta_{eg})] \tag{5a}$$

and

$$\mathrm{Re}[\dot{\delta}_{eg}]+\gamma_2\,\mathrm{Re}[\delta_{eg}]\cong-\dot{\theta}\,\mathrm{Im}[\langle\sigma_{eg}\rangle]. \tag{5b}$$

We will return to this specific small-signal assumption subsequently.

Substituting from Eq. (3b) into Eq. (5b) then yields

$$\mathrm{Re}[\delta_{eg}]\cong-\frac{1}{2}\frac{m\Omega\gamma_2}{[\gamma_2^2+\Delta^2+(\gamma_2/\gamma_1)\Omega^2]}\sin(\omega_m t), \tag{6}$$

and after substituting Eq. (6) into Eq. (5a), we get for the modulated probability of finding the atom in the excited state (i.e., $p\equiv\delta_{ee}$),

$$\ddot{p}+\gamma_1\dot{p}+\Omega^2 p=-\frac{1}{2}\left[\frac{\Omega^2 m\omega_m\Delta}{\gamma_2^2+\Delta^2+(\gamma_2/\gamma_1)\Omega^2}\right]\cos[\omega_m t]-\frac{1}{4}\left[\frac{m^2\omega_m\Omega^2\gamma_2}{\gamma_2^2+\Delta^2+(\gamma_2/\gamma_1)\Omega^2}\right]\sin[2\omega_m t]. \tag{7}$$

As is readily apparent, Eq. (7) is the equation of a damped harmonic oscillator, driven by two sinusoidal forcing functions. The solution of Eq. (7) can therefore be written as the sum of two oscillating probabilities, $p_\alpha+p_\beta$, which individually obey damped, driven, harmonic oscillator equations:

$$\ddot{p}_\alpha+\gamma_1\dot{p}_\alpha+\Omega^2 p_\alpha=-\frac{1}{2}\left[\frac{\Omega^2 m\omega_m\Delta}{\gamma_2^2+\Delta^2+(\gamma_2/\gamma_1)\Omega^2}\right]\cos[\omega_m t], \tag{8a}$$

$$\ddot{p}_\beta+\gamma_1\dot{p}_\beta+\Omega^2 p_\beta=-\frac{1}{4}\left[\frac{m^2\omega_m\Omega^2\gamma_2}{\gamma_2^2+\Delta^2+(\gamma_2/\gamma_1)\Omega^2}\right]\sin[2\omega_m t]. \tag{8b}$$

The solutions of Eqs. (8) are, of course, well known [14] so that we get finally,

$$p_\alpha(t)=-\frac{1}{2}\left[\frac{\Omega^2 m\omega_m\Delta}{\gamma_2^2+\Delta^2+(\gamma_2/\gamma_1)\Omega^2}\right]\frac{\sin(\omega_m t+\phi_\alpha)}{\sqrt{(\Omega^2-\omega_m^2)^2+\gamma_1^2\omega_m^2}}, \tag{9a}$$

$$p_\beta(t)=\frac{1}{4}\left[\frac{m^2\omega_m\Omega^2\gamma_2}{\gamma_2^2+\Delta^2+(\gamma_2/\gamma_1)\Omega^2}\right]\frac{\cos(2\omega_m t+\phi_\beta)}{\sqrt{(\Omega^2-4\omega_m^2)^2+4\gamma_1^2\omega_m^2}}, \tag{9b}$$

where $\phi_\alpha=\tan^{-1}[(\Omega^2-\omega_m^2)/\gamma_1\omega_m]$ and $\phi_\beta=\tan^{-1}[(\Omega^2-4\omega_m^2)/2\gamma_1\omega_m]$. Thus, the amplitudes of each of the oscillating terms exhibit resonance when the Rabi frequency equals either ω_m, in the case of p_α, or $2\omega_m$, in the case of p_β. Since the p_α and p_β oscillating probabilities may be experimentally distinguished, we refer to the resonant behavior of their amplitudes as the α and β Rabi resonances, respectively.

As our primary interest is in the β Rabi resonance (i.e., $\Delta=0$ and $\Omega=2\omega_m$) due to its atomic candle application, Eq. (4b) yields for $\mathrm{Im}[\delta_{eg}]$ in this case,

$$\mathrm{Im}[\dot{\delta}_{eg}]+\gamma_2\,\mathrm{Im}[\delta_{eg}]=\dot{\theta}\,\mathrm{Re}[\delta_{eg}]-\Omega p_\beta. \tag{10}$$

Substituting from Eqs. (6) and (9b), this then yields

$$\mathrm{Im}[\dot{\delta}_{eg}]+\gamma_2\,\mathrm{Im}[\delta_{eg}]\approx\left[\frac{m^2\Omega}{8}\right]\sin(2\omega_m t+\psi). \tag{11}$$

Consequently, for conditions associated with the β Rabi resonance (i.e., $\gamma_2\ll\Omega\sim 2\omega_m$), we expect $|\mathrm{Im}[\delta_{eg}]|\sim m^2/8$. Considering the specific small-signal approximation that we invoked above, this is to be compared with $\mathrm{Im}[\langle\sigma_{eg}\rangle]\sim\gamma_1/2\Omega_0=\gamma_1/4\omega_m$. Consequently, the small-signal approximation may be viewed as a constraint on the magnitude of the modulation index, such that we require $m<\sqrt{2\gamma_1/\omega_m}$.

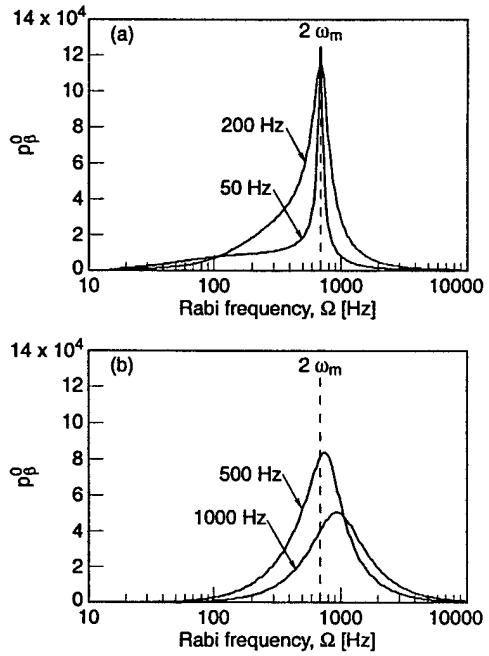

FIG. 1. Line shapes of the β Rabi resonance for the case where $\gamma_1=\gamma_2$. (a) Fast modulation, where $\omega_m \gg \gamma_1, \gamma_2$; this is the regime of the theory's validity and the line shapes correspond to $\gamma_1/2\pi=50$ and 200 Hz. (b) Regime of slow modulation, and the line shapes correspond to $\gamma_1/2\pi=500$ and 1000 Hz.

For signal-to-noise considerations, our experiment has necessarily violated this constraint to some degree. Nonetheless, as will be discussed below, our experimental results are in good agreement with the small-signal theory, suggesting that this condition on the modulation index may not be overly constraining on the theory's validity.

B. The β-Rabi-resonance line shape

As is clear from Eqs. (9), when $\Delta=0$ the oscillatory behavior of $p(t)$ is considerably simplified, since only the β resonance then has any significance. Writing $p_\beta(t)=p_\beta^0\cos(2\omega_m t+\phi_\beta)$, we obtain

$$p_\beta^0=\frac{1}{4}\frac{m^2\omega_m\Omega^2\gamma_2\left[\gamma_2^2+\left(\frac{\gamma_2}{\gamma_1}\right)\Omega^2\right]^{-1}}{\sqrt{(\Omega^2-4\omega_m^2)^2+4\gamma_1^2\omega_m^2}}. \tag{12}$$

This resonance line shape of p_β^0 as a function of the Rabi frequency is illustrated in Fig. 1 for the case $\omega_m/2\pi=350$ Hz and $m=0.1$. As is clearly shown in Fig. 1(a) for the case of fast modulation (i.e., $2\omega_m \gg \gamma_1, \gamma_2$), p_β^0 displays a resonant increase when $\Omega=2\omega_m$, with a peak amplitude of $m^2/8$. In Fig. 1(b) we display the theory's predictions in the case where the modulation is not rapid, and though certainly suspect in this regime, we note for latter qualitative comparison with experiment that the line shape of the β Rabi resonance broadens and its peak shifts to higher Rabi frequencies.

C. Linewidth of the β Rabi resonance

To determine the half-width half-maximum, $\delta\Omega_{1/2}$, of the β resonance, we define $\delta\Omega_{1/2}$ as $|\Omega-2\omega_m|$ and set $p_\beta^0(\delta\Omega_{1/2})=m^2/16$ in Eq. (12). In this way, it is straightforward to show under conditions of fast modulation that

$$\delta\Omega_{1/2}=\pm 2\omega_m\left[\sqrt{1\pm\frac{\sqrt{3}}{2}\frac{\gamma_1}{\omega_m}}-1\right]\cong\frac{\sqrt{3}}{2}\gamma_1. \tag{13}$$

This result has interesting implications for the atomic candle, since the candle's instability as defined through its Allan standard deviation, $\sigma_{\Delta P/P}(\tau)$ [15], is inversely proportional to the β-resonance line Q (i.e., $\Omega_0/2\delta\Omega_{1/2}$) [16]. In previous work we verified that $\Omega_0=2\omega_m$ for the β resonance [13], so that Eq. (13) then yields

$$Q=\frac{2\omega_m}{\gamma_1\sqrt{3}}\Rightarrow\sigma_{\Delta P/P}\sim\frac{\gamma_1}{\omega_m}. \tag{14}$$

Thus, the stability of the atomic candle in this approximation has the potential to be improved greatly by simply designing the device to work at ever higher modulation frequencies.

D. Inhomogeneous broadening

In many experiments, such as the one to be described below, the field will not be uniform over the atomic sample volume, but will have some modal distribution. Consequently, if the atoms are unable to sample the field's spatial distribution on the time scale of a Rabi period, then the β Rabi resonance will be inhomogeneously broadened. Specifically, as the average field intensity is changed for fixed ω_m, different spatial regions within the signal volume will go into and out of the β-resonance condition. To account for inhomogeneous broadening, we write the observed dynamic response of a sample as the weighted average of atomic responses throughout the signal volume. Specifically, in the case of inhomogeneous broadening, $p_\beta^0(\Omega)$ becomes a functional of $\Omega(\vec{r})$, and the observed line shape of the β Rabi resonance, $L_\beta(\bar{\Omega})$, becomes

$$L_\beta(\bar{\Omega})=\int p_\beta^0(\Omega)W(\vec{r})d^3\vec{r}, \tag{15}$$

where $\bar{\Omega}$ is the average Rabi frequency over the signal volume and $W(\vec{r})$ is a spatial weighting function that describes how strongly a spatial region contributes to the integrated Rabi-resonance signal.

In the experiment to be described below, we optically pump a sample of alkali atoms contained within a cylindrical TE_{011} microwave cavity, in this way creating a population imbalance between the atom's ground-state hyperfine levels. As our beam diameter is relatively small compared to the cavity radius, we need only consider the axial spatial variations, so that for the spatial variation of the Rabi frequency we have

$$\Omega(z)=\Omega_{\text{peak}}\sin\left(\frac{\pi z}{L}\right), \tag{16}$$

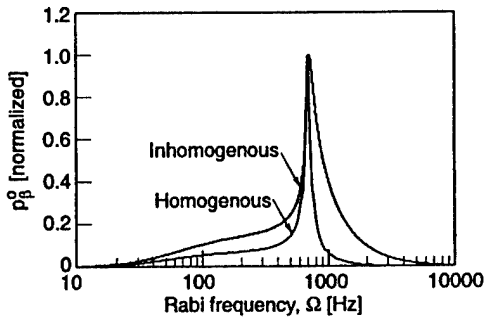

FIG. 2. Influence of inhomogeneous broadening on the line shape of the β Rabi resonance for a total longitudinal relaxation rate (including the effect of optical pumping) of 50 Hz, $\omega_m/2\pi = 350$ Hz, and $m=0.1$. Additionally, for this specific example we choose an optical depth ζ^{-1} of 10 cm and a cavity length L of 5 cm.

where L is the cavity length. Though the weighting function $W(z)$ is determined by a complicated interplay between atomic diffusion to the resonance cell walls, where the hyperfine population imbalance is destroyed by wall collisions [17], and the exponential attenuation of the optical pumping rate due to Beer's law absorption in the alkali vapor, for the purposes of the present discussion we consider $W(z)$ to be reasonably well approximated as the simple product of two terms. The first term describes the local "microscopic" influence of various parameters on the signal, most notably the optical pumping rate, while the second term accounts for the macroscopic variation of the signal associated with spatial diffusion [18,19], which for simplicity we assume to be well described by the first-order diffusion mode [i.e., $\sin(\pi z/L)$]:

$$W(z)=\left[\frac{\Gamma_{abs}e^{-\zeta z}}{\Gamma_{abs}e^{-\zeta z}+4\gamma_1}\right]\sin\left(\frac{\pi z}{L}\right). \tag{17}$$

Here, Γ_{abs} is the photon absorption rate at the front of the resonance cell and ζ^{-1} is the vapor's optical depth. Clearly, we should only expect this empirical weighting function to be valid in alkali vapors that are not too optically thick and for relatively slow optical pumping rates. Figure 2 provides an example of the effect of inhomogeneous broadening on the line shape of the β Rabi resonance for a case where the total longitudinal relaxation rate is 50 Hz and again $\omega_m/2\pi = 350$ Hz. (When optical pumping is included, $\gamma_1 \approx \gamma_{col} + 0.5\Gamma_{abs}$, where γ_{col} is the relaxation rate due to all collisional processes including, phenomenologically, diffusion, so that for Fig. 2 we set $\gamma_{col}/2\pi = 25$ Hz and $\Gamma_{abs}/2\pi = 50$ Hz.) We note that there is a slight broadening and shift of the line shape, with the resonant Rabi frequency changing from 700 to 716 Hz or by $\approx +2\%$.

III. EXPERIMENT

Figure 3 shows a block diagram of our experimental arrangement. Light from a diode laser is tuned to the Rb^{87} D_1 transition at 794.7 nm [i.e., $5\,^2S_{1/2}(F=2)$-$5\,^2P_{1/2}(F'=1)$], attenuated by neutral density filters, and then expanded and apertured to a final diameter of 0.8 cm. (Given the 520-MHz Doppler broadening of the optical transition, we are just able

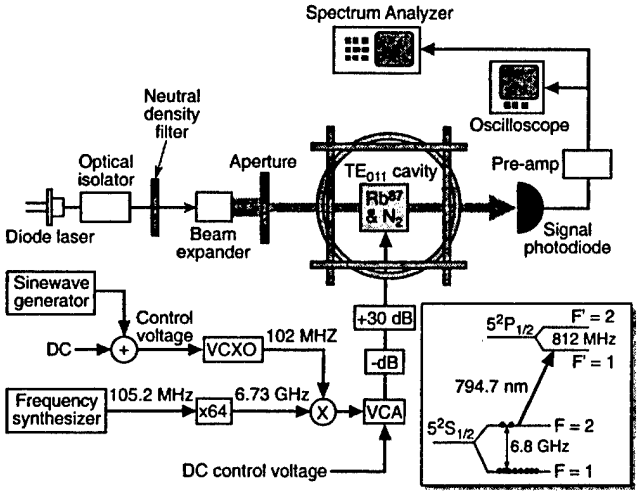

FIG. 3. Block diagram of the experimental arrangement as described in the text.

to resolve the 812-MHz excited hyperfine splitting between the $F'=1$ and $F'=2$ hyperfine states.) The laser beam passes into a resonance cell containing isotopically enriched Rb^{87} along with 10-torr N_2, which is housed in a cylindrical TE_{011} microwave cavity resonant with the ground-state hyperfine transition at 6834.7 MHz. The Corning 7070 resonance cell fits snugly into the cavity, and has a length of 5.6 cm, a diameter, $2R$, of 5.7 cm, and is heated with braided windings wrapped on the cavity body to about 45 °C corresponding to a Rb vapor density of $\sim 10^{11}$ cm^{-3} [20]. The cavity and cell are centrally located in a set of three mutually perpendicular Helmholtz coils: two pairs zero out the Earth's residual magnetic field, while the third provides a quantization axis for the atoms (i.e., the z axis) parallel to the laser propagation direction and cavity symmetry axis, $B_{z,dc}$ ~ 400 mG. Transmission of the light through the vapor is monitored with a Si photodiode.

In the absence of microwaves resonant with the $(F=2, m_F=0)$-$(1,0)$ hyperfine transition (i.e., 0-0 transition), depopulation optical pumping reduces the density of atoms in the $F=2$ absorbing state [21], and consequently increases the amount of light transmitted through the vapor. However, when the resonant microwave signal is present, atoms return to the $F=2$ state, thereby reducing the amount of transmitted light. The transmitted laser intensity thus acts as a measure of atomic population in the $F=2$ level, so that any microwave induced oscillation of this population will be observed as oscillations in the transmitted light and will appear as a bright line on the spectrum analyzer. We note that Doppler broadening plays no role in the microwave resonance as a consequence of Dicke narrowing [22].

The microwaves are derived from a very low phase noise frequency synthesizer, whose output at 105.2 MHz is multiplied up into the microwave regime and then mixed with the output of a voltage-controlled crystal oscillator (VCXO) at ~ 102 MHz. The microwaves are attenuated by the combination of a voltage-controlled attenuator (VCA) and a fixed attenuator (labeled as $-$dB in the figure) before being amplified by a +30-dB solid-state amplifier. A sinusoidal signal of

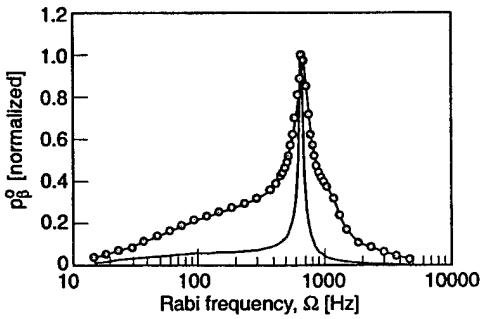

FIG. 4. Experimental line shape of the β Rabi resonance for $I=8\ \mu\mathrm{W/cm^2}$, $\omega_m/2\pi=328$ Hz, and $m=0.74$. The solid line corresponds to the theoretical line shape of Eq. (12) for $\gamma_1/2\pi=28.6$ Hz.

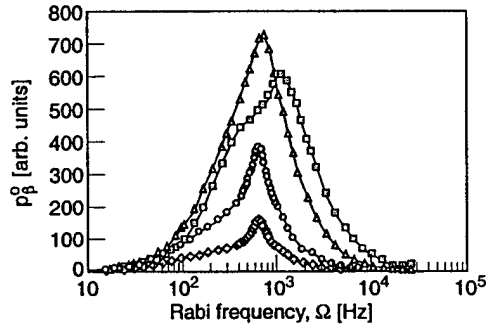

FIG. 5. Experimental line shapes of the β Rabi resonance as a function of laser intensity with $\omega_m/2\pi=328$ Hz and $m=0.74$: diamonds correspond to 30 $\mu\mathrm{W/cm^2}$, circles correspond to 56 $\mu\mathrm{W/cm^2}$, triangles correspond to 249 $\mu\mathrm{W/cm^2}$, and squares correspond to 457 $\mu\mathrm{W/cm^2}$.

frequency ω_m is added to a dc voltage in order to provide the VCXO's control voltage V_c. The dc level of V_c tunes the average microwave frequency to the 0-0 hyperfine resonance, while the sine wave provides microwave frequency (i.e., phase) modulation.

In our experiment, the N_2 buffer gas "freezes" the atoms in place on the time scale of a typical Rabi period, so that the atoms experience local values of the microwave magnetic field's z component: $B_z(\rho,z)=B_{\mathrm{peak}}J_0(3.8\rho/R)\sin(\pi z/L)$. Since we probe the center of the TE_{011} cavity with our laser, the Bessel function term is essentially unity, so that any inhomogeneity in our Rabi-resonance line shapes will be dominated by the axial variation of B_z.

We calibrated our microwave attenuators to Ω using the linewidth $\Delta\nu$ of the slow-passage 0-0 line shape [23]. Though the measurement can be problematic due to the cavity's modal field distribution, at very low microwave power levels it can be shown that this linewidth is a good measure of the *peak* Rabi frequency in the cavity (i.e., $\Delta\nu\Rightarrow\mu B_{\mathrm{peak}}/\hbar$) [24]. We therefore used very low light intensities ($\sim 2\ \mu$W) to avoid light-shift effects on the line shape [25], and measured the 0-0 hyperfine transition width as a function of the microwave attenuation level. A least-squares fit of the data then provided the attenuator calibration. Using the slow-passage linewidth measurements we also determined our collisional dephasing rate γ_{col} and optical pumping rate (i.e., $0.5\Gamma_{\mathrm{abs}}$), finding $\gamma_{\mathrm{col}}/2\pi\cong 25$ Hz and $\Gamma_{\mathrm{abs}}/2\pi=\kappa I$, where I is the laser intensity in $\mu\mathrm{W/cm^2}$ and $\kappa\sim 0.9\ \mathrm{Hz}/(\mu\mathrm{W/cm^2})$.

The procedure for obtaining the line shapes of the β Rabi resonance was relatively straightforward. With the microwave average frequency close to the 0-0 hyperfine resonance, we set our fixed attenuator so as to maximize the second-harmonic atomic signal as observed on the spectrum analyzer. At this power level, we then fine tuned the microwave frequency by making the first harmonic signal zero. The line shapes were obtained by changing the fixed attenuator setting in combination with the VCA voltage, and measuring the second-harmonic atomic signal amplitude per $\sqrt{\mathrm{Hz}}$ with the spectrum analyzer. Since the microwave attenuation setting was calibrated to the Rabi frequency, this procedure gave p^0_β as a function of Ω.

Figure 4 is an example of our β-Rabi-resonance line shape for $I=8\ \mu\mathrm{W/cm^2}$, $\omega_m/2\pi=328$ Hz, and $m=0.74$. The filled circles are the experimental data while the black solid curve corresponds to Eq. (12) using the experimental estimates of γ_{col} and Γ_{abs}. In this particular example, we have $\sqrt{2\gamma_1/\omega_m}=0.63$, so that we do not quite meet the small-signal theory's constraint on modulation index. Nevertheless, the experimental data's agreement with the small-signal theory is quite good, considering that the experimental line shape is inhomogeneously broadened. In this regard, referring back to Fig. 2, we note that the experimental line shape is broader than the theoretical homogeneous line shape and that the experimental line shape appears to be shifted very slightly (if at all) to a higher Rabi frequency. Specifically, though we measure a 3% shift of the resonance to a higher Rabi frequency, our experimental uncertainty of the resonance's peak position is $\pm 5\%$ [13].

Figure 5 illustrates the behavior of the β-resonance line shapes as a function of light intensity for $\omega_m/2\pi=328$ Hz and $m=0.74$: diamonds correspond to 30 $\mu\mathrm{W/cm^2}$ (i.e., $\gamma_1/2\pi=\gamma_{\mathrm{col}}/2\pi+0.5\Gamma_{\mathrm{abs}}/2\pi=39$ Hz), circles correspond to 56 $\mu\mathrm{W/cm^2}$ ($\gamma_1/2\pi=50$ Hz), triangles correspond to 249 $\mu\mathrm{W/cm^2}$ ($\gamma_1/2\pi=137$ Hz), and squares correspond to 457 $\mu\mathrm{W/cm^2}$ ($\gamma_1/2\pi=231$ Hz). As the light intensity increases, the amplitude of the line shape increases, since the increased rate of optical pumping produces larger population imbalances and hence larger modulation amplitudes. However, consistent with Fig. 1(a), for $\gamma_1\ll\omega_m$ the β-resonance condition remains fixed at $2\omega_m$ and the line shape simply broadens with the increase in relaxation rate. In the regime of slow modulation, consistent with Fig. 1(b), we see that there is a further broadening of the line shape accompanied by a shift in resonance to a higher Rabi frequency.

Of the small-signal theory's predictions, probably the two most significant are (1) that the β Rabi resonance's amplitude increases like m^2, and (2) that the line Q increases with increasing modulation frequency. Figure 6 shows the amplitude of the β resonance as a function of the modulation index for $\omega_m/2\pi=328$ Hz and $I=8\ \mu\mathrm{W/cm^2}$. The solid curve is a least-squares power-law fit to the data and yields $p^0_\beta\sim m^{(1.95\pm 0.05)}$. Figure 7 shows the line shape of the β Rabi resonance for two different modulation frequencies with $I=5\ \mu\mathrm{W/cm^2}$ and $m=0.74$: circles correspond to $\omega_m/2\pi$

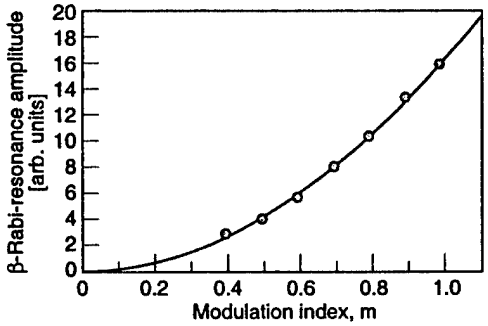

FIG. 6. Amplitude of the β Rabi resonance as a function of the modulation index: $\omega_m/2\pi=328$ Hz and $I=8$ μW/cm^2.

$=328$ Hz, while diamonds correspond to $\omega_m/2\pi=1$ kHz. In addition to the shift of the β resonance from about 650 Hz to 2 kHz, the higher modulation frequency line shape appears narrower on the log plot. This appearance is a manifestation of the line shape's higher line Q. In an effort to examine this observation more quantitatively, we fit the peak portions of the line shapes (i.e., normalized $p_\beta^0>0.7$) to Lorentzians. (As we had no quantitative theory for the *inhomogeneous* line shape, we felt that a Lorentzian fit to the peak portion would be the least biased.) In this way we determined that $Q_{328}\cong 4.1$ and $Q_{1000}\cong 7.9$. Consistent with the small-signal theory we find an increase in line Q with modulation frequency. Though we only see a factor of 2 increase in line Q, while theory would predict a factor of 3 increase for the specific change in modulation frequency, we attribute this discrepancy to the inhomogeneous broadening of the line shape of the β Rabi resonance.

IV. DISCUSSION

When an atom interacts with a phase-modulated field, the atom responds by oscillating between its excited state and its ground state. The amplitude of these oscillations displays a resonant enhancement when the Rabi frequency takes on specific values, and these resonant enhancements are termed Rabi resonances. Here, we considered a small-signal theory of the Rabi-resonance phenomena and demonstrated the existence of two different types of resonance, the α Rabi resonance and the β Rabi resonance. Given the β resonance's

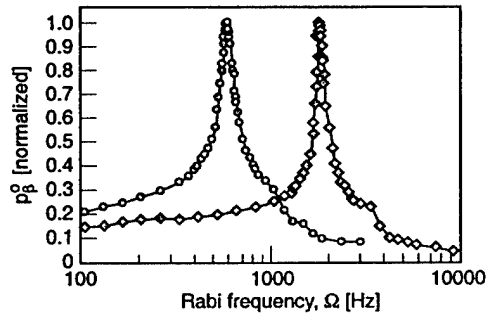

FIG. 7. Experimental line shapes of the β Rabi resonance for two different modulation frequencies: circles correspond to $\omega_m/2\pi=328$ Hz, while diamonds correspond to $\omega_m/2\pi=1$ kHz. For these experiments, $I=5$ μW/cm^2 and $m=0.74$.

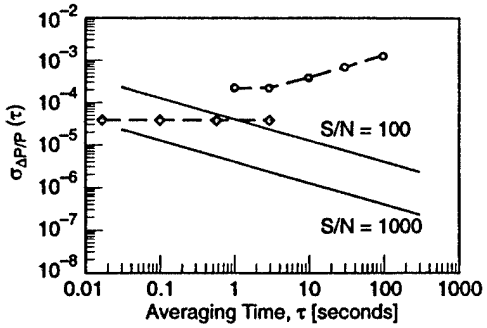

FIG. 8. Predicted intensity stability of a field stabilized by a optical atomic candle based on the cesium D_1 transition's (894.6 nm) β Rabi resonance. The dashed line connecting open diamond corresponds to the Allan standard deviation of a free-runnin single-mode diode laser as measured in Ref. [26], while the dashe line connecting open circles corresponds to the Allan standard de viation of a free-running diode laser as measured in Ref. [27].

application in the area of atomic candles, our work focuse on the line shape of this particular Rabi resonance. Experi mentally, we found that the small-signal theory was quit accurate in predicting the shape of the β resonance, and o particular relevance is the fact that we found that the line (of the β resonance has the theoretical potential for very larg values. This result is significant, since it suggests the possi bility of employing very narrow β Rabi resonances fo atomic candle operation, and thereby the production of field with ultrastable intensity in the long term.

Given the present work's validation of the small-signa line-shape theory, it is possible to address the question o how stable an atomic candle's output field might conceivabl be. Specifically, if a *laser* was stabilized using the β-Rabi resonance phenomenon, what type of optical intensity stabil ity could one hope to achieve? For simplicity, we consider situation in which the (not insignificant) issue of Dopple broadening is ignored, and we assume that the line shape o the β Rabi resonance is homogeneously broadened. Unde these idealized conditions, it is straightforward to show tha the relative (white noise) intensity fluctuations of the can dle's output field, $\sigma_{\Delta P/P}$, will be given by $2\delta\Omega_{\rm rms}/\Omega_0$ where $\delta\Omega_{\rm rms}$ is the root-mean-square deviation of the Rab frequency averaged over some time interval τ and Ω_0 is th nominal Rabi frequency. Assuming a standard feedback loo for the atomic candle [16], we therefore expect

$$\sigma_{\Delta P/P}(\tau)\approx\frac{2}{Q(S/N)}\frac{1}{\sqrt{\tau}}, \tag{18}$$

where (S/N) is the signal-to-noise ratio in a 1-Hz bandwidt and τ is in seconds.

As a specific example, we consider an optical candle op erating on the cesium D_1 line, so that $\gamma_1/2\pi=4.6$ MHz, an we consider laser phase modulation at a 2-GHz rate; fro Eq. (14) we therefore have a β-Rabi-resonance line Q of 50 Figure 8 plots $\sigma_{\Delta P/P}$ as a function of τ for this exampl assuming signal-to-noise ratios of 10^2 and 10^3. We note th

in our experiment, signal-to-noise ratios in a 1-Hz bandwidth were on the order of 10^2. Since the locked Rabi frequency in this example would be 4 GHz, the laser would have to emit 100 mW of power focused into a 100-μm-diameter beam. For comparison, Fig. 8 also shows the Allan standard deviation of a free-running single-mode diode laser as measured by Tsuchida and Tako (diamonds) [26] and Yamaguchi and Suzuki (circles) [27]. Clearly, there is the potential for creating very stable fields using an atomic candle, with the specific advantage that these fields would exhibit long-term stability.

As a final point, it is interesting to note from Eq. (4) that with regard to optical β Rabi resonances, both the Rabi frequency and longitudinal decay rate due to spontaneous emission depend on the transition's electric dipole moment μ_{eg}. Consequently,

$$Q_{\text{opt}}=\frac{\sqrt{3}c^3E_0}{4\omega_{eg}^3\mu_{eg}}, \tag{19}$$

where ω_{eg} is the resonant optical frequency and E_0 is the optical field strength. Thus, the highest β-resonance line-Q transitions, and therefore the most stable optical atomic candles (not considering issues of signal-to-noise ratio), will be those based on weak infrared transitions employing very strong fields.

ACKNOWLEDGMENTS

The authors thank S. Moss and B. Jaduszliwer for readings of the manuscript and several stimulating discussions. This work was supported by the U.S. Air Force Space and Missile Systems Center under Contract No. F04701-00-C-0009.

[1] See, for example, R. Karplus, Phys. Rev. **73**, 1027 (1948); R. Arndt, J. Appl. Phys. **36**, 2522 (1965); J. Vanier and C. Audoin, *The Quantum Physics of Atomic Frequency Standards* (Institute of Physics, Bristol, 1989), Vol. 2, Chap. 5.

[2] M. Nakazawa, J. Appl. Phys. **59**, 2297 (1986).

[3] Y. Kayanuma, Phys. Rev. B **47**, 9940 (1993); B. M. Garraway and N. V. Vitanov, Phys. Rev. A **55**, 4418 (1997); W. Harshawardhan and G. S. Agarwal, *ibid.* **55**, 2165 (1997); Y. Kayanuma and Y. Mizumoto, *ibid.* **62**, 061401(R) (2000).

[4] R. P. Frueholz, Phys. Rev. A **61**, 023805 (2000).

[5] S. Papademetriou, S. Chakmakjian, and C. R. Stroud, J. Opt. Soc. Am. B **9**, 1182 (1992).

[6] M. W. Noel, W. M. Griffith, and T. F. Gallagher, Phys. Rev. A **58**, 2265 (1998).

[7] C. Audoin, V. Candelier, and N. Dimarcq, IEEE Trans. Instrum. Meas. **40**, 121 (1991); J. Q. Deng, G. Mileti, R. E. Drullinger, D. A. Jennings, and F. L. Walls, Phys. Rev. A **59**, 773 (1999); R. Barillet, F. Hamouda, D. Venot, and C. Audoin, IEEE Trans. Instrum. Meas. **47**, 1152 (2000); M. Ortolano, N. Beverini, and A. De Marchi, *ibid.* **47**, 471 (2000).

[8] J. C. Camparo, J. G. Coffer, and R. P. Frueholz, Phys. Rev. A **56**, 1007 (1997); **58**, 3873 (1998).

[9] J. C. Camparo, Phys. Rev. Lett. **80**, 222 (1998).

[10] J. G. Coffer and J. C. Camparo, Phys. Rev. A **62**, 013812 (2000).

[11] J. C. Camparo, in *Proceedings of the 1998 IEEE International Frequency Control Symposium*, edited by J. R. Vig (IEEE, Piscataway, NJ, 1998), pp. 88–94.

[12] T. Swan-Wood, J. G. Coffer, and J. C. Camparo, IEEE Trans. Instrum. Meas. **50**, 1229 (2001).

[13] J. C. Camparo and J. G. Coffer (unpublished).

[14] K. R. Symon, *Mechanics* (Addison-Wesley, Reading, MA, 1971), Chap. 2.

[15] D. W. Allan, IEEE Trans. Instrum. Meas. **36**, 646 (1987).

[16] See, for example, J. Vanier and L.-G. Bernier, IEEE Trans. Instrum. Meas. **30**, 277 (1981).

[17] P. Minguzzi, F. Strumia, and P. Violino, Nuovo Cimento **46B**, 145 (1966); F. A. Franz, Phys. Rev. A **6**, 1921 (1972).

[18] J. C. Camparo and R. P. Frueholz, J. Appl. Phys. **59**, 301 (1986).

[19] J. C. Camparo and R. P. Frueholz, J. Appl. Phys. **59**, 3313 (1986); IEEE Trans. Ultrason. Ferroelectr. Freq. Control **34**, 607 (1987).

[20] T. J. Killian, Phys. Rev. **27**, 578 (1926).

[21] W. Happer, Rev. Mod. Phys. **44**, 169 (1972).

[22] R. H. Dicke, Phys. Rev. **89**, 472 (1953); R. P. Frueholz and C. H. Volk, J. Phys. B **18**, 4055 (1985).

[23] J. C. Camparo and R. P. Frueholz, Phys. Rev. A **31**, 1440 (1985).

[24] J. C. Camparo and R. P. Frueholz, Phys. Rev. A **30**, 803 (1984).

[25] J. C. Camparo, R. P. Frueholz, and C. H. Volk, Phys. Rev. A **27**, 1914 (1983).

[26] H. Tsuchida and T. Tako, Jpn. J. Appl. Phys., Part 1 **22**, 1152 (1983).

[27] S. Yamaguchi and M. Suzuki, IEEE Trans. Instrum. Meas. **36**, 789 (1987).